Pharmaceutical Research, Vol. 26, No. 8, August 2009 (© 2009)
DOI: 10.1007/s11095-009-9894-2

Research Paper

Formulation and Pharmacokinetics of Self-Assembled Rifampicin Nanoparticle Systems for Pulmonary Delivery

Jean C. Sung,[1] Danielle J. Padilla,[2] Lucila Garcia-Contreras,[2] Jarod L. VerBerkmoes,[1] David Durbin,[3] Charles A. Peloquin,[3] Katharina J. Elbert,[1] Anthony J. Hickey,[2] and David A. Edwards[1,4]

Received February 4, 2009; accepted April 11, 2009; published online April 30, 2009

Purpose. To formulate rifampicin, an anti-tuberculosis antibiotic, for aerosol delivery in a dry powder 'porous nanoparticle-aggregate particle' (PNAP) form suited for shelf stability, effective dispersibility and extended release with local lung and systemic drug delivery.
Methods. Rifampicin was encapsulated in PLGA nanoparticles by a solvent evaporation process, spray dried into PNAPs containing varying amounts of nanoparticles, and characterized for physical and aerosol properties. Pharmacokinetic studies were performed with formulations delivered to guinea pigs by intratracheal insufflation and compared to oral and intravenous delivery of rifampicin.
Results. The PNAP formulations possessed properties suitable for efficient deposition in the lungs. *In vitro* release showed an initial burst of rifampicin, with the remainder available for release beyond eight hours. PNAPs delivered to guinea pigs by insufflation achieved systemic levels of rifampicin detected for six to eight hours. Moreover, rifampicin concentrations remained detectable in lung tissue and cells up to and beyond eight hours. Conversely, after pulmonary delivery of an aerosol without nanoparticles, rifampicin could not be detected in the lungs at eight hours.
Conclusions. Our results indicate that rifampicin can be formulated into an aggregated nanoparticle form that, once delivered to animals, achieves systemic exposure and extends levels of drug in the lungs.

KEY WORDS: aerosols; antibiotics; nanoparticles; pulmonary drug delivery; tuberculosis.

INTRODUCTION

Tuberculosis (TB) continues to be a leading cause of death due to infectious disease worldwide, even though adequate treatments are available. Nearly one-third of the world's population is infected with *Mycobacterium tuberculosis*, the microbe that causes TB in a latent or active form, while more than eight million people develop active TB every year and nearly two million people die annually from TB (1). Tuberculosis is an infectious disease spread through inhalation of airborne droplets containing *M. tuberculosis* (2) and subsequent uptake of the bacterium by alveolar macrophages (3). Treatment of tuberculosis is an arduous and lengthy process requiring combination antibiotic therapy administered daily for at least six months (4). During this extended therapy, patients may terminate treatment early due to factors such as unwanted side effects or alleviation of primary symptoms (5). Partial treatment of TB can make the disease more difficult to treat since selection of drug-resistant mutants of *M. tuberculosis* may occur. Thus, an advance in TB therapy that reduces frequency of dosing, body dose and overall treatment time has the potential to be more effective, thereby saving lives.

An obvious strategy for reducing the treatment dose of antibiotics for TB treatment involves the steady delivery of antibiotic to infected cellular tissue. Compared to the current approach to therapy (4), whereby antibiotics are delivered without targeting of infected cells and without sustaining drug levels above therapeutic thresholds, a targeted extended delivery of antibiotics can potentially reduce dosing frequency and overall treatment time simultaneously. A current obstacle to extended release formulation of antibiotics for TB is the relatively large daily antibiotic dose (gram quantities) required for TB treatment. This high body dose is particularly needed given the oral and parenteral routes of delivery, since drugs reach target tissues through the systemic circulation, i.e., while distributing throughout the body. Delivering antibiotics directly to the lungs increases local drug concentrations while allowing for systemic exposure

[1] Harvard School of Engineering and Applied Sciences, 29 Oxford Street, Pierce 322, Cambridge, Massachusetts 02138, USA.
[2] School of Pharmacy, University of North Carolina at Chapel Hill, Kerr Hall, Chapel Hill, North Carolina 27599, USA.
[3] National Jewish Medical and Research Center, Denver, Colorado 80206, USA.
[4] To whom correspondence should be addressed. (e-mail: dedwards@seas.harvard.edu)

ABBREVIATIONS: BAL, Bronchoalveolar lavage; DCM, Dichloromethane; FPF_{TD}, Fine particle fraction of the total dose less than 5.8 μm; NP, Nanoparticles; PK, Pharmacokinetics; PLGA, Poly (lactide-*co*-glycolide); PNAP, Porous nanoparticle-aggregate particle; PNAP40, PNAPs containing 40% NP by weight; PNAP80, PNAPs containing 80% NP by weight; PP, Porous particles; PVA, Poly(vinyl alcohol); TB, Tuberculosis.

[through transport across lung epithelia (6,7)] for treatment of non-pulmonary TB in a non-invasive manner. Targeting extended release formulations of the drug to the lungs, the primary site of infection, may then result in a lower systemic dose, reduced frequency of dosing and shortened treatment times compared to standard oral or systemic treatment alone to achieve the desired therapeutic effect.

Delivery of drugs to the lungs in sustained release formulations requires the encapsulation of drugs in microparticle or nanoparticle structures. A need to target the immune system, including phagocytic cells and ultimately the systemic circulation, suggests that aerosol particles containing TB antibiotics should possess an aerodynamic size of approximately 1 to 4 μm, suitable for relatively deep lung penetration in humans (8). Even larger particles can be delivered if they are sufficiently light or porous, and, indeed, such porous particles (PP) are particularly effective at dispersing in a dry powder form and penetrating the lungs—even from simple, low-cost, and easy-to-use inhaler systems (9). The application of porous particles to treat tuberculosis has been investigated with the tuberculostatic agents para-aminosalicyclic acid (PAS) (10) and capreomycin (11,12).

Nanoparticle formulations are a particularly interesting approach to sustained delivery in the lungs given the avid uptake of nanoparticles by macrophages and other cells of the immune system (13,14). Previously they have been used to deliver drugs to the lungs by nebulization (15–17). Nebulization, the delivery by aerosol of liquid formulations via sonication and other forms of liquid aerosol cloud generation, poses several challenges to practical implementation in the case of TB. Long delivery times, low delivery efficiencies, stability of sustained-release formulations in aqueous solution and access to clean water are a few of these challenges (18,19). Drying nanoparticles and delivering as a dry powder is not easily achieved given that nanoparticles aggregate excessively in the dry state (20,21). Alternatively, nanoparticles delivered in unaggregated dry particle form are generally exhaled from the lungs owing to their low inertia (8,22).

A novel approach to sustained-release aerosol formulations that addresses these issues involves the creation of a micron-scale porous particle composed of self-assembled biodegradable nanoparticles that delivers the nanoparticles effectively to the lungs (23,24). We have developed these 'porous nanoparticle-aggregate particles' (PNAPs) to act as carrier particles that release the nanoparticles from the aggregate once delivered into the body, acting as "Trojan" delivery systems for nanoparticles that would, otherwise, not deposit in the lungs in a dry form. The PNAP can be composed entirely of nanoparticles or the nanoparticles can be dispersed throughout a matrix of inert pharmaceutical excipient, such as leucine, a hydrophobic amino acid previously demonstrated to improve powder dispersibility and aerosolization properties (25,26).

In the present study, we investigated whether PNAPs could be designed for delivery of an antibiotic for the treatment of tuberculosis. Previous work with PNAPs has been reported for small molecules including the lung cancer therapeutic doxorubicin (27), salbutamol sulfate and aspirin (28), and the protein insulin (29). While *in vitro* testing has appeared promising, the PNAP delivery system has, until now, not been demonstrated as a viable drug delivery system for relatively large quantities of drugs or nanoparticles with *in vivo* testing.

We chose rifampicin, a first-line drug given orally to treat TB, as our model drug. Rifampicin was formulated for aerosol delivery into both a porous particle formulation without nanoparticles and a PNAP form incorporating varying amounts of nanoparticles formed from the biocompatible polymer poly(lactide-*co*-glycolide) (PLGA). These powders were characterized to confirm that they possessed desirable physical and aerodynamic properties suitable for deposition in the lungs. The powders were then delivered to guinea pigs by intratracheal insufflation and drug concentrations were determined in plasma, lung lining fluid, via bronchoalveolar lavage (BAL), and lung tissue homogenates.

MATERIALS AND METHODS

Materials

L-leucine and rifampicin were obtained from Spectrum Chemicals & Laboratory Products (Gardena, CA). Rifampicin is an orange red powder, slightly soluble in water (~1.3 g/l) and soluble in methyl and ethyl alcohol. Poly(vinyl alcohol) (PVA, MW 13,000–23,000, 87–89% hydrolyzed) was purchased from Sigma-Aldrich (St. Louis, MO) and poly(dl-lactide-*co*-glycolide) (PLGA; Medisorb®, 50:50 lactide/glycolide ratio, inherent viscosity 0.16 dL/g, MW ~14,000) was supplied by Alkermes (Cincinnati, OH). Acetonitrile, ethanol USP grade and methanol were purchased from Pharmco Products Inc. (Brookfield, CT). Dichloromethane (DCM) was obtained from Mallinckrodt (Phillipsburg, NJ). Water from a Millipore Corp. (Billerica, MA) Milli-Q water purification system was used.

Preparation of PNAPS

Nanoparticle Preparation

Rifampicin-containing nanoparticles (NP) were prepared using a solvent evaporation method. PLGA, 3.84 g, was dissolved in 96.0 ml of DCM. Rifampicin, 3.84 g, was added to this solution, and the solution was agitated until dissolution of materials. An aliquot of this solution, 2.00 ml, was added to an aqueous solution containing 6.00 ml of 1% PVA. An emulsion was formed using a VibraCell sonicator (Sonics and Materials, Newtown, CT). The emulsion was transferred to a 0.1% PVA solution and allowed to stir overnight for removal of DCM. This procedure was repeated for the remainder of the polymer and drug solution. The nanoparticles were collected by centrifugation (10,000 × *g* for 30 min) and washed twice with fresh water to remove residual PVA and drug. The nanoparticle concentration in suspension was assessed by lyophilizing aliquots of the solution and weighing afterwards.

Spray Drying Liquid Feed Preparation

The spray drying liquid feed was prepared by dissolving L-leucine in water. The desired amount of nanoparticle

suspension was then added to this and allowed to stir. Formulations containing 40% nanoparticles by weight (PNAP40) were prepared using 3.20 g leucine, 2.10 g nanoparticles and 0.54 L water, while formulations containing 80% nanoparticles by weight (PNAP80) used 0.60 g leucine, 2.40 g nanoparticles and 0.30 L water. Ethanol was measured into a separate vessel: 0.80 L for the 40% NP formulation and 0.45 L for the 80% NP formulation.

PNAP Dry Powder Formation

Porous particles containing nanoparticles (40% or 80% NP by weight) were prepared using a Niro, Inc. Mobile Minor spray dryer (Columbia, MD). The inlet temperature was set at 84–87°C and the liquid feed rate at a total of 50 ml/min. The leucine-nanoparticle aqueous suspension was separate from the organic phase and mixed in-line immediately prior to atomization. The liquid feed was pumped into the two-fluid nozzle of the spray dryer with a gas flow rate of 25 g/min and nozzle pressure of 40 psi. Spray dried powders were collected in a container at the outlet of the cyclone.

Preparation of Porous Particles

Spray Drying Solution Preparation

The spray drying solution was prepared by dissolving 1.20 g of L-leucine and 0.80 g of rifampicin in 0.20 L of water. Then 0.30 L of ethanol was added to this mixture, while stirring. The solution was agitated until dissolution of all materials.

Porous Particle Formation

Porous particles (PP) were prepared using a Niro, Inc. Mobile Minor spray dryer (Columbia, MD). The inlet temperature was set at 95°C and the solution feed rate at 50 ml/min. The solution was pumped into the two-fluid nozzle of the spray dryer with a gas flow rate of 25 g/min and nozzle pressure of 33 psi. Spray dried powders were collected in a container at the outlet of the cyclone.

Particle Characterization

Characterization of Nanoparticles

The size and polydispersity index (PdI) of the nanoparticles were assessed by photon correlation spectroscopy (or dynamic light scattering) using a ZetaSizer Nano ZS (Malvern Instruments Inc., Southborough, MA). The prepared nanoparticle solution was diluted in fresh water and measured at 20°C. The reported size was the Z-average size (or "cumulants mean") as calculated from the intensity, and the PdI was a width parameter also calculated from the cumulants analysis of the signal intensity. The nanoparticle zeta potential was also determined with this instrument.

Characterization of Dry Powders

The volume median diameter of the spray dried powder was measured by laser diffraction using a HELOS system with RODOS dry dispersing unit (Sympatec Inc., Lawrenceville, NJ) at an applied pressure of 2 bar. Each determination was performed in triplicate on a given powder.

An eight-stage Andersen non-viable 1ACFM Cascade Impactor (ACI) (Copley Scientific Limited, Nottingham, UK) was used to determine the aerodynamic particle size distribution of the powder. Capsules (HPMC, Size 3; Shionogi Qualicaps, Madrid, Spain) were approximately half-filled with powder (where PNAP40 contained 11.5±0.1 mg, PNAP80 10.4±0.1 mg and PP 3.9±0.2 mg powder) and placed in a hand-held, dry powder breath-activated inhaler device (Plastiape, Osnago, Italy). The capsule was punctured and the powder was drawn through the cascade impactor operated at a flow rate of 28.3 L/min for 4.2 s, simulating an inspiration. The aerosolized powder deposited on glass fiber filters at each stage of the impactor depending upon the particles' aerodynamic diameter. The filters were weighed before and after each experiment. The fine particle fraction of the total dose of powder less than or equal to an effective cut-off aerodynamic diameter of 5.8 μm (FPF_{TD}) was calculated by dividing the powder mass recovered from stages 1–7 of the impactor by the total particle mass in the capsule. The geometric standard deviations (GSD) of dry powders were determined from:

$$\mathrm{GSD} = (d_{84\%}/d_{16\%})^{0.5}$$

where d_n is the diameter at the nth percentile of the cumulative distribution.

The dry particles were viewed using scanning electron microscopy (SEM). A LEO 982 field emission scanning electron microscope (Carl Zeiss, Inc., Thornwood, NY) was operated at 2 kV with a filament current of about 0.5 mA. Powder samples were prepared by deposition on a double-coated carbon conductive tape tab (Ted Pella Inc., Redding, CA) mounted on a pin mount and dusted. The sample was then coated with a Platinum/Palladium layer with a Cressington Scientific Instruments Inc. (Watford, UK) 208HR sputter coater, operated for 60 s at a sputtering current of 40 mA.

Drug Load of Powders

The rifampicin load of the spray dried powder was determined by a modified reverse-phase high performance liquid chromatography (HPLC) method (30) using an Agilent 1100 Series HPLC system with C_{18} column (Zorbax) and ChemStation software (Agilent Technologies Inc., Palo Alto, CA). The mobile phase was run on a linear gradient from 45% 0.02 M phosphate buffer, 41% methanol and 14% acetonitrile to 25% 0.02 M phosphate buffer, 56% methanol and 19% acetonitrile over 20 min plus 10 min at the final composition and a 5 min post run. Analysis was performed on a 10 μL injection at a flow rate of 1.0 ml/min through an Agilent Zorbax Eclipse XDB-C18 (4.6×150 mm) column and absorbance recorded at 337 nm. An Agilent Zorbax Eclipse XDB-C18 analytical guard column was also used.

Residual PVA Content

Residual poly(vinyl alcohol) (PVA) content of nanoparticles was assayed by UV spectroscopy of its complex with

iodine in the presence of boric acid (31). The nanoparticle PLGA matrix was dissolved in dichloromethane, followed by extraction of PVA by dissolution in water. The PVA was then complexed with iodine in the presence of boric acid. Absorbance at 298 K and 649 nm was measured utilizing a SpectraMax M2 microplate reader (Molecular Devices Corp., Sunnyvale, CA) and concentration of PVA determined by comparison with a standard curve prepared under identical conditions.

In vitro Release Studies

In vitro release of rifampicin from the different particle systems was tested under sink conditions using a modified dissolution method (30). A 0.05 M phosphate buffer solution at pH 7.2 was used, with the addition of 200 μg/ml ascorbic acid acting as an antioxidant to prevent oxidative degradation of rifampicin. A known mass of powder was suspended in bottles containing buffer solution. Three replicates were performed for each powder. The jars were placed on a magnetic stirplate at 37°C. Aliquots were taken from the jars at selected time intervals and centrifuged. The supernatant was removed and analyzed by HPLC. The resulting drug concentration in solution was converted to a percentage of the total initial drug amount and plotted as cumulative percent release over time.

Pharmacokinetic Studies

Experimental Design

Male Dunkin-Hartley guinea pigs weighing 456.6±95.4 g were employed in pharmacokinetic (PK) studies. Animals were housed in a 12 h light/12 h dark cycle and constant temperature environment of 22°C. A standard diet of food and water were supplied *ad libitum*. All animal procedures were approved by the Institutional Animal Care and Use Committee (IACUC) of the University of North Carolina at Chapel Hill in accordance with "Principles of Laboratory Animal Care" (NIH publication #85–23, revised in 1985). Before the study, each animal underwent cannulation of the right external jugular vein for continuous blood sampling and allowed to recover overnight (32).

Animals were randomly divided into five groups, respectively, receiving rifampicin as follows: intravenously (IV) in solution at a dose of 10 mg/kg, orally as a suspension using an oral gavage needle at a dose of 2.5 mg/kg, and as dry powder via intratracheal insufflation (Penn Century, Philadelphia, PA) by the pulmonary route in three forms. Insufflated powders included porous powders (PP) at a nominal dose of 2.5 mg/kg, PNAPs containing 40% nanoparticles (PNAP40) at a nominal dose of 2.5 mg/kg and PNAPs containing 80% nanoparticles (PNAP80) at nominal doses of 2.5 and 4 mg/kg. These doses were based on the practical limitations of delivering large masses of dry powders to the guinea pigs. Blood samples (0.35 ml) were collected from each animal into heparinized tubes with ascorbic acid at 0, 0.08, 0.25, 0.5, 1.0, 1.5, 2, 3, 4, 6 and 8 h. Sterile saline solution was used to replace the blood volume lost through sample collection. Plasma was separated and stored at −80°C until analysis. After collection of the last blood sample, animals were anesthetized and euthanized by exanguination, and bronchoalveolar lavage (BAL) was conducted (5 ml sterile saline). The BAL sample was centrifuged and the pellet and supernatant separated and stored separately at −80°C. Finally, lung tissues were collected from the animals to determine local drug concentration.

Sample Analysis

Plasma and BAL samples (pellet and supernatant) were analyzed by a validated HPLC assay for drug content (33). Serum concentrations of rifampicin were determined using a system consisting of a ThermoFinnegan P4000 HPLC pump (San Jose, CA) with model AS1000 fixed-volume autosampler, a model UV2000 ultraviolet detector, a Gateway Series e computer (Poway, CA) and the Chromquest HPLC data management system. The plasma standard curve for rifampicin ranged from 0.05 to 5.0 μg/ml. The absolute recovery of rifampicin from plasma was 103%. The overall validation precision across all standards was 1.43% to 4.56%. Sample preparation for the BAL pellets and supernatants were adaptations of the plasma method for the specific matrix in question, with identical HPLC methods.

Pharmacokinetic Analysis

Pharmacokinetic parameters of total area under the curve $\left[\mathrm{AUC}_{(0-\infty)}\right]$, dose-normalized total area under the curve $\left[\mathrm{AUC}_{(0-\infty)}/\mathrm{dose}\right]$, mean residence time (MRT), half-life ($t_{1/2}$), the elimination rate constant (K) and clearance (CL/F) were obtained by non-compartmental analysis methods using WinNonlin (Pharsight Corporation, Mountain View, CA). Maximum rifampicin concentrations ($C_{\max}$) and time to obtain the maximum rifampicin concentration ($T_{\max}$) were determined from the non-fitted plasma *versus* time profiles for each individual animal. Bioavailability (F) was calculated by the following equation:

$$F = \frac{\mathrm{AUC}_{\mathrm{lung,\ oral}}}{\mathrm{AUC}_{\mathrm{IV}}} \times \frac{D_{\mathrm{IV}}}{D_{\mathrm{lung,\ oral}}}$$

where D is the dose and subscripts refer to routes of administration: intravenous (IV), pulmonary (lung), and oral.

Statistical Analysis

Data for the pharmacokinetic study was subjected to analysis of variance (ANOVA) and the least-squares significant-differences multiple comparison method, Student–Newman–Keuls. A probability level of 5% ($p<0.05$) was considered to be statistically significant.

RESULTS

Particle Design and Characterization

We prepared particles containing 40% and 80% nanoparticles by weight (PNAP40 and PNAP80 respectively) with similar physical and aerosol characteristics. The volume median diameter of the PNAPs was 4.2±0.1 μm for PNAP40

and 4.2±0.1 μm for PNAP80, as determined by laser diffraction. Both powders exhibited properties suitable for deposition in the respiratory tract with FPF_{TD}=35.5±2.1% and 44.7±2.3% for PNAP40 and PNAP80, respectively. Rifampicin contents of the two powders scaled linearly with the amount of nanoparticles; thus, PNAP40 contained 5.2±0.1% rifampicin and PNAP80 10.0±0.1% rifampicin. Scanning electron microscopy showed that the PNAP had a thin-walled structure composed of visible aggregated nanoparticles, as shown in Fig. 1.

Both PNAP40 and PNAP80 were composed of nanoparticles of Z-average size 195±4 nm and a PdI of 0.06±0.01, as measured by photon correlation spectroscopy of the signal intensity. The nanoparticles contained a rifampicin content of 13.5±0.9%. Zeta potential of the particles was −33.0±1.8 mV and PVA content of the nanoparticles was 2.0%. Electron microscopy of the lyophilized nanoparticles showed spherical structures with smooth surfaces (Fig. 2).

To ascertain the effect of the nanoparticles on delivery and release, porous particles without nanoparticles were prepared containing rifampicin within the matrix. The spray dried formulation produced thin-walled particle structures as shown in Fig. 3. The volume median diameter of the particles was 2.7±0.1 μm, with desirable aerosol properties indicated by a FPF_{TD}=67.8±0.5%. The rifampicin content of the powder was measured to be 39.1±0.3%.

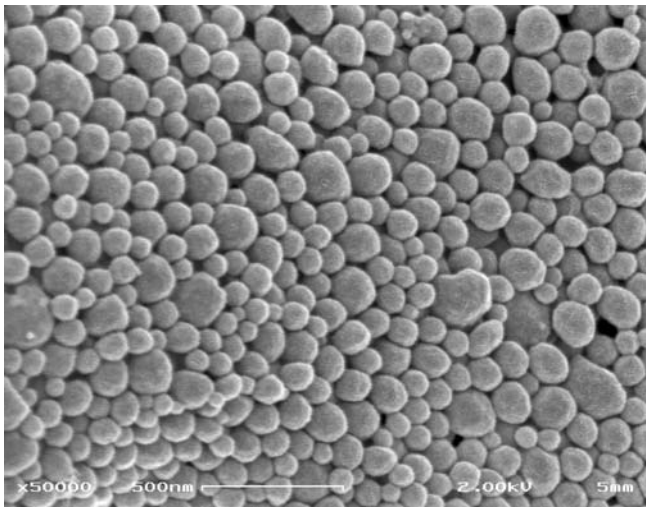

Fig. 2. Scanning electron micrograph of lyophilized rifampicin PLGA nanoparticles (NP) (scale bar represents 500 nm).

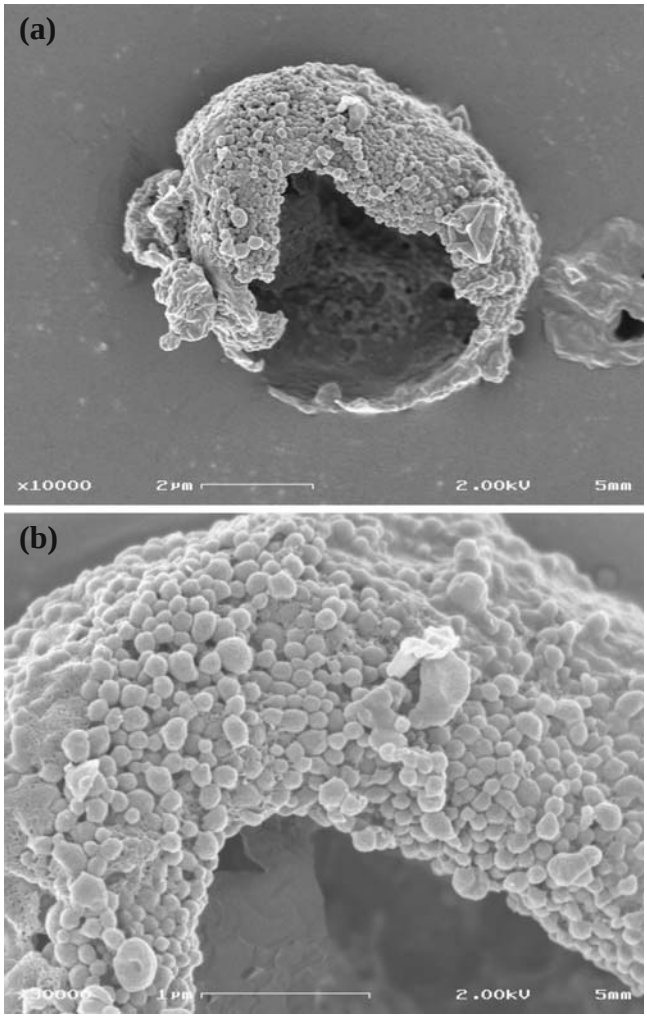

Fig. 1. Scanning electron micrographs of spray dried rifampicin porous particle containing 80% nanoparticles by weight (PNAP80). A magnification of the surface of the PNAP indicates a shell of aggregated nanoparticles with structure intact (scale bars represent: **a** 2 μm, **b** 1 μm).

In vitro Release Studies

In vitro release studies were performed with the PNAP and PP formulations and pure crystalline rifampicin. The release profiles showed a burst release of approximately 80% of drug content almost immediately, with the remainder available for release over a period beyond eight hours (Fig. 4).

Pharmacokinetic Studies

The *in vitro* antibiotic release profile of PNAP formulations coincides with systemic absorption of drug that is comparable to the PP control without nanoparticles. Plots of average rifampicin plasma concentration *versus* time following delivery of our dry powder formulations to guinea pigs are shown in Fig. 5. While plasma levels revealed statistical differences between insufflated groups and IV (not shown) or oral treatment at all time points, the insufflated (with or without nanoparticles) groups at the 2.5 mg/kg dose demonstrated no significant differences in average rifampicin plasma concentrations at the various time points. This may be a reflection of the *in vitro* release profile (Fig. 4), which shows an early burst of drug nearing 80% of the rifampicin content, after which little difference exists between the various formulations for many hours. Consistent with a higher dose, the PNAP80 formulation dosed at 4 mg/kg exhibited significantly higher concentrations at the earlier time points than at a dose of 2.5 mg/kg, without dose correction. Conversely, rifampicin concentrations in the lungs remained elevated for all PNAP formulations – unlike the IV, oral and PP insufflated groups (Fig. 6). This was observed both in BAL and lung tissue.

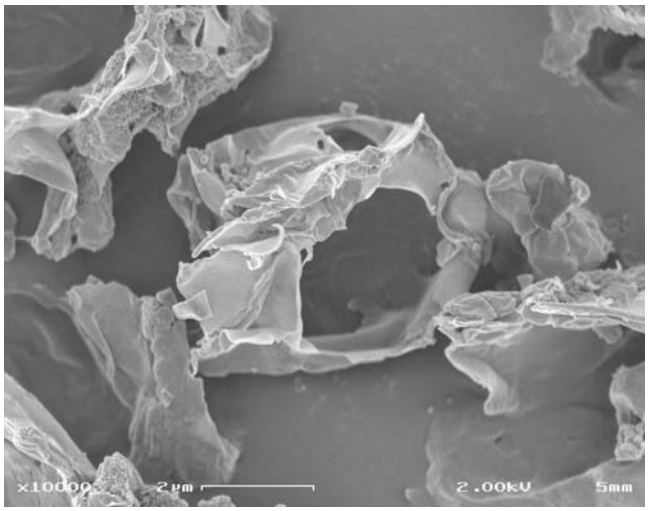

Fig. 3. Scanning electron micrograph of spray dried rifampicin porous particles (PP) (scale bar represents 2 μm).

PK parameters obtained by non-compartmental methods are presented in Table I. Total area under the curve $\left[AUC_{(0-\infty)}\right]$, dose-corrected AUC $\left[AUC_{(0-\infty)}/dose\right]$, mean residence time (MRT), half-life ($t_{1/2}$) and the elimination rate constant (K) were comparable among animals in all insufflated groups at the dose of 2.5 mg/kg. Of the insufflated groups, PNAP80 (4 mg/kg) demonstrated the highest AUC and C_{max}, and the longest MRT, consistent with a higher rifampicin dose. It is likely that the MRT of PNAP80 at 4 mg/kg was different than that of PNAP80 at 2.5 mg/kg due to differences in drug solubility in the lung environment. Dose-normalized AUCs of all pulmonary formulations were significantly higher than that of the oral treatment, although direct comparison of only the pulmonary formulations did not reach statistical significance. The formulations PNAP40 (2.5 mg/kg) and PNAP80 (4 mg/kg) demonstrated the highest bioavailabilities of F ~0.72 and ~0.73, respectively, while the oral treatment (2.5 mg/kg) had the lowest bioavailability of F ~0.17.

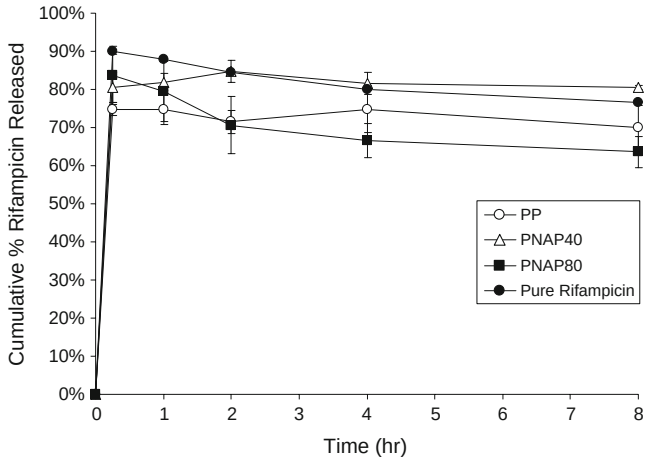

Fig. 4. Drug release profile of rifampicin in phosphate buffer medium (0.05 M, pH 7.2, with 200 μg/ml ascorbic acid) from porous particles (*open circle*), nanoparticle aggregate systems containing 40% rifampicin nanoparticles by weight (*open triangle*) or 80% rifampicin nanoparticles by weight (*filled square*), and pure rifampicin (*filled circle*) (mean±standard deviation, n=3).

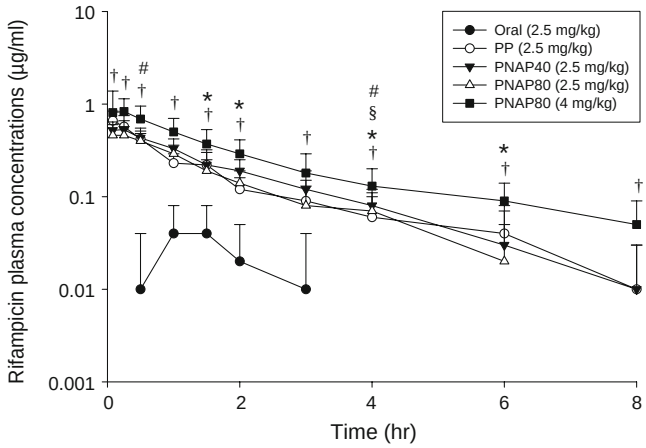

Fig. 5. Average rifampicin plasma concentration *versus* time curves after administration of rifampicin to guinea pigs in suspension orally (oral) at 2.5 mg/kg and in formulation at the following treatments and doses by insufflation: rifampicin porous particles (PP) at 2.5 mg/kg, porous particles containing 40% rifampicin nanoparticles by weight (PNAP40) at 2.5 mg/kg and porous particles containing 80% rifampicin nanoparticles by weight (PNAP80) at both 2.5 mg/kg and 4 mg/kg (mean±standard deviation, n=4–10). While no significant difference was seen in average plasma concentrations amongst the different formulations delivered by insufflation at a dose of 2.5 mg/kg (PP, PNAP40, PNAP80), all of the insufflated powders resulted in significantly higher average plasma concentrations than the oral rifampicin. $^{\#}P<0.05$: PP *vs.* PNAP80 (4 mg/kg); $^{\S}P<0.05$: PNAP40 (2.5 mg/kg) *vs.* PNAP80 (4 mg/kg); $^{*}P<0.05$: PNAP80 (2.5 mg/kg) *vs.* PNAP80 (4 mg/kg); $^{\dagger}P<0.05$: oral *vs.* PP, PNAP40 (2.5 mg/kg), PNAP80 (2.5 mg/kg) and PNAP80 (4 mg/kg).

DISCUSSION

The continued threat of tuberculosis and issues with disease management due to patient non-compliance motivate investigations for an improved therapy that could reduce

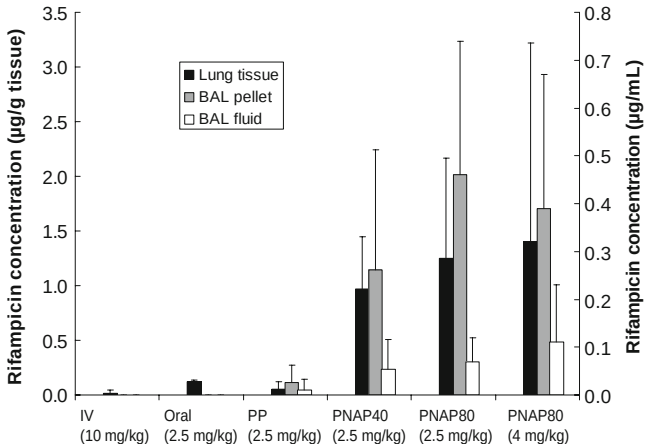

Fig. 6. Rifampicin concentrations in homogenized lung tissue and bronchoalveolar lavage (BAL) components (supernatant and pellet resulting from centrifugation of the BAL fluid) from guinea pigs 8 h post-treatment. While 8 h after dosing, low or no levels of rifampicin were found in the lung tissue or BAL results for insufflated porous particles or rifampicin given intravenously or orally, those formulations containing nanoparticles (PNAP40, PNAP80) showed extended levels of rifampicin in the lungs (mean±standard deviation, n=4–9). Drug levels in the BAL pellet indicate uptake of drug by lung cells such as macrophages or intact particles remaining in the lungs.

Table I. Plasma Pharmacokinetic Parameters Obtained by Non-compartmental Analysis After Administration of Various Rifampicin Treatments by Different Routes of Administration (Mean±Standard Deviation, n=4–10)

	Treatments					
Parameter	IV (10 mg/kg)	Oral (2.5 mg/kg)	PP (2.5 mg/kg)	PNAP40 (2.5 mg/kg)	PNAP80 (2.5 mg/kg)	PNAP80 (4 mg/kg)
$AUC_{(0-\infty)}$ (μgh/ml)	7.44±1.06	0.31±0.09[a]	1.06±0.38[a,b]	1.33±0.28[a,b]	0.98±0.34[a,b]	2.16±0.52[a,b,c,d,e]
$AUC_{(0-\infty)}/dose$	0.74±0.11	0.12±0.04[a]	0.43±0.15[a,b]	0.53±0.11[a,b]	0.39±0.13[a,b]	0.54±0.13[a,b]
K (h^{-1})	0.56±0.05	0.31±0.15	0.46±0.28	0.41±0.22	0.50±0.26	0.28±0.19
$t_{1/2}$ (h)	1.24±0.12	2.63±1.16	2.26±1.63	2.37±1.64	1.78±0.95	3.79±2.47
MRT (h)	1.81±0.20	1.31±0.46	1.50±0.50	1.66±0.60	1.37±0.39	2.20±0.45[e]
CL/F (ml h^{-1} kg^{-1})	1.37±0.22	8.62±2.93[a]	2.68±1.08	1.97±0.53[b]	2.85±1.06	1.96±0.52[e]
C_{max} (μg/ml)	3.88±0.58	0.08±0.02[a]	0.67±0.18[b]	0.57±0.12[a,b]	0.50±0.11[a,b]	1.05±0.46[b,e]
T_{max} (h)	0.12±0.09	1.00±0.5	0.19±0.14	0.18±0.09	0.21±0.15	0.26±0.29
$F_{(0-\infty)}$	–	0.17±0.05	0.57±0.21[b]	0.72±0.15[b]	0.53±0.18[b]	0.73±0.18[b,e]

$AUC_{(0-\infty)}$ total area under the curve (time zero to infinity), $AUC_{(0-\infty)}/dose$ dose-normalized total area under the curve (time zero to infinity), K elimination rate constant, $t_{1/2}$ half-life, MRT mean residence time, CL/F clearance, C_{max} maximum concentration, T_{max} time at which C_{max} occurs, F bioavailability

[a] Significantly different from IV

[b] Significantly different from oral

[c] Significantly different from PP

[d] Significantly different from PNAP40 (2.5 mg/kg)

[e] Significantly different from PNAP80 (2.5 mg/kg)

dosing frequency, shorten treatment length and reduce side effects. One such treatment is a drug delivery system that sustains release of drugs and targets the primary site of action, the lungs. Rifampicin and other antitubercular drugs have been investigated in polymeric particle form for inhalation as both microparticles (34–37) and nanoparticles (38–41). These studies have shown that treatment with nebulized or insufflated particles containing antibiotics is effective in decreasing bacterial counts in infected animals with reduced doses. The goal of our study was to evaluate the potential utility of nanoparticle aggregate drug delivery systems that would allow rapid delivery to the lungs as a dry powder via a simple inhaler.

PLGA nanoparticles encapsulating rifampicin were prepared by a solvent evaporation process that resulted in particles with low polydispersity and relatively high drug loading. These nanoparticles were spray dried into PNAPs incorporating various amounts of nanoparticles into the porous particle form. These final particles were characterized to have desirable aerosol properties for efficient lung deposition with nanoparticle loadings up to 80% by weight. The small nanoparticle size and relatively high drug loading led to rather rapid *in vitro* release of the majority of rifampicin, with the remaining approximately 20% of drug available for release beyond eight hours, as has been seen previously with drugs encapsulated in nanoparticles (42).

PLGA is a biocompatible and biodegradable polymer with a growing body of data to support its safety in the lungs. Studies have shown PLGA to have no overt toxicity in healthy lung macrophages when in microparticle form (37) and to not induce pulmonary inflammation when delivered to mice in nanoparticle form (43). While the experimental formulation explored in this study would not be delivered on a daily basis and PLGA nanoparticles have been shown to decrease rapidly in molecular weight over the first week of exposure to PBS (44), it is possible that some polymer may remain in the lungs. However, the addition of drug may hasten degradation of the polymer and lung clearance mechanisms, such as macrophage uptake or mucociliary clearance, may remove residual polymer from the lungs. The fate of PLGA nanoparticles in the lungs will have to be explored further. Furthermore, other polymers may be explored to target specific polymer degradation times and to tailor drug release profiles.

The pharmacokinetic study performed with the rifampicin formulations indicated sustained levels of drug in the lungs after treatment with PNAPs at doses of 2.5 and 4.0 mg/kg of rifampicin. The normal adult human dose for oral rifampicin is 600 mg once daily or approximately 10 mg/kg, with reported bioavailability of F=0.68, although F is known to be highly variable across a population (45,46). Ideally, the rifampicin dosage in this study would have been correlated with human dosage or calculated on the surface area of the animal, however rifampicin doses in this study had to be based upon the maximum amount of powder that could be tolerated by the guinea pigs. Also, free drug was not administered via the pulmonary route as a control, since it was not possible to deliver free rifampicin of the appropriate particle size for effective dispersion.

Reflective of the *in vitro* release profile, a relatively rapid release of rifampicin was seen *in vivo* (as evidenced by the rapid appearance of drug in the plasma). However, the formulation of rifampicin into nanoparticles led to prolonged rifampicin presence in the lungs up to eight hours after delivery. Differences were seen between dry powders with and without nanoparticles, where PP showed much lower rifampicin levels in the lung tissue and BAL components than the PNAP formulations, indicating evidence for delayed release from the nanoparticles. Moreover, PNAP80 formulations showed higher BAL pellet and lung tissue concentrations than PNAP40. Since phagocytosis of nanoparticles of the size used in this study typically occurs within a few hours following deposition, and given the aerodynamic properties of the PNAPs (designed to deliver a significant fraction of

drug to the deep lungs), it is likely that the rifampicin levels observed in the guinea pig lungs at eight hours reflect either drug associated with alveolar macrophages or that intact particles remain in the lungs. This may be implicit in the elevated rifampicin concentrations in the lung tissue and BAL pellet *versus* the BAL fluid. The variability between the lung tissue and BAL results for the PP and PNAP formulations may be due to the difference in aerosol properties of the powders, potentially resulting in different deposition patterns that may have contributed to different dissolution times among the particle systems. Future work may include microscopic evaluation of the fate of the PNAPs in the lungs (*e.g.*, macrophage uptake or intact particles). However, these results do suggest that PNAP powders are an effective system for delivering nanoparticle extended release drug formulations to the lungs in a dry powder form conducive to simple and inexpensive delivery.

It is also worth noting that rifampicin plasma concentrations after pulmonary administration of PNAPs to guinea pigs were higher at all times and had longer plasma concentration *versus* time profiles than after the standard oral administration of equivalent doses of rifampicin suspension at 2.5 mg/kg, which was also reflected in the AUC and the bioavailability of the drug (AUC~0.98 to 2.16 *versus* AUC~0.21; *F*~0.53 to 0.72 *versus* *F*~0.17). Furthermore, corrected by dose, the AUC for pulmonary administration of particle formulations was significantly higher than that of the oral rifampicin treatment (~0.39 to 0.54 *versus* ~0.12). Oral rifampicin at higher doses in humans (10 mg/kg) is known to have a higher bioavailability (*F*~0.68) (45,46). These higher doses in humans may saturate either gastrointestinal efflux pumps, such as P-glycoprotein, or clearance pathways, such as biliary clearance (47), however that saturation has not been observed at these doses in guinea pigs (32). In this study, it is likely that the low oral bioavailability was the result of the low dose and potentially due to efficiency of delivery of that dose. Overall, the higher bioavailability by the pulmonary route is a promising sign for obtaining systemic exposure to rifampicin.

The MIC values of rifampicin against *M. tuberculosis* range from 0.025 to 0.2 μg/ml (45,46). The C_{max} concentrations reached by the insufflated groups were within the range of the MIC, although by 8 h the concentrations were at or just below the lower limit of the MIC. The residual amount of PNAP-loaded rifampicin in the lung tissue and BAL indicates the potential for a delayed release of undissolved drug in the lungs that may be available for therapeutic treatment. Future work may explore delivering larger amounts of rifampicin to the lungs by ways such as increasing drug load in nanoparticles.

Our results indicate an approach to formulate TB drugs for pulmonary delivery where frequency of dosing and daily dose of drug required can both be lowered, given the demonstrated high systemic exposure on dosing and elevated lung levels between dosing. It is envisioned that the aerosol delivery of drug would accompany standard oral delivery to provide these advantages of reduced dosing frequency, shortened treatment length and reduced side effects. Future work should explore the treatment of TB by pulmonary delivery of PNAPs containing rifampicin, and other antibiotic drugs, to demonstrate the therapeutic advantages of this drug delivery form.

CONCLUSIONS

We have shown that drug can be formulated into an aggregated nanoparticle form using biocompatible materials and with aerosol properties suitable for lung deposition. Once delivered to animals, these PNAPs both deliver drug systemically and extend levels of drug in the lungs for up to eight hours. This drug delivery system has the potential to provide therapeutic advantages for diseases where both systemic and local treatment of the lungs may improve treatment, such as tuberculosis.

ACKNOWLEDGEMENTS

The authors thank Plastiape for their generous donation of inhaler devices and Shionogi for supplying capsules, Prof. Patrick Couvreur for fruitful discussions and Annalicia Poehler for research assistance. Electron microscopy work was performed at the Center for Nanoscale Systems (CNS), part of the Faculty of Arts and Sciences at Harvard University. This work was supported by a grant from the National Institute of Health/NIAID under Grant Number 5 U01 61336-02 and a National Science Foundation Graduate Research Fellowship.

REFERENCES

1. WHO. Tuberculosis fact sheet. Geneva: World Health Organization; 2006.
2. Riley RL, Mills CC, Nyka W, Weinstock N, Storey PB, Sultan LU, *et al.* Aerial dissemination of pulmonary tuberculosis: a two-year study of contagion in a tuberculosis ward. Am J Epidemiol 1959;70:185–96.
3. Russell DG. Mycobacterium tuberculosis: here today and here tomorrow. Nat Rev Mol Cell Biol 2001;2:569–86. doi:10.1038/35085034.
4. Fox W, Ellard GA, Mitchison DA. Studies on the treatment of tuberculosis undertaken by the British Medical Research Council Tuberculosis Units, 1946–1986, with relevant subsequent publications. Int J Tuberc Lung Dis 1999;3:S231–79.
5. Thomas C. A literature review of the problems of delayed presentation for treatment and non-completion of treatment for tuberculosis in less developed countries and ways of addressing these problems using particular implementations of the DOTS strategy. J Manage Med 2002;16:371–400. doi:10.1108/02689230210446544.
6. Patton JS. Mechanisms of macromolecule absorption by the lungs. Adv Drug Deliv Rev 1996;19:3–36.
7. Patton JS, Fishburn CS, Weers JG. The lungs as a portal of entry for systemic drug delivery. Proc Am Thorac Soc 2004;1:338–44. doi:10.1513/pats.200409-049TA.
8. Heyder J, Gebhart J, Rudolf G, Schiller CF, Stahlhofen W. Deposition of particles in the human respiratory tract in the size range 0.005–15 um. J Aerosol Sci 1986;17:811–25. doi:10.1016/0021-8502(86)90035-2.
9. Edwards DA, Hanes J, Caponetti G, Hrkach J, Ben-Jebria A, Eskew ML, *et al.* Large porous particles for pulmonary drug delivery. Science 1997;276:1868–72. doi:10.1126/science.276.5320.1868.
10. Tsapis N, Bennett D, O'Driscoll K, Shea K, Lipp MM, Fu K, *et al.* Direct lung delivery of para-aminosalicylic acid by aerosol particles. Tuberculosis 2003;83:379–85. doi:10.1016/j.tube.2003.08.016.
11. Fiegel J, Garcia-Contreras L, Thomas M, VerBerkmoes J, Elbert K, Hickey A, *et al.* Preparation and *in vivo* evaluation of a dry powder for inhalation of capreomycin. Pharm Res 2007;25:805–11.

12. Garcia-Contreras L, Fiegel J, Telko MJ, Elbert K, Hawi A, Thomas M, *et al.* Inhaled large porous particles of capreomycin for treatment of tuberculosis in a guinea pig model. Antimicrob Agents Chemother 2007;51:2830–6. doi:10.1128/AAC.01164-06.
13. Gelperina S, Kisich K, Iseman MD, Heifets L. The potential advantages of nanoparticle drug delivery systems in chemotherapy of tuberculosis. Am J Respir Crit Care Med 2005;172:1487–90. doi:10.1164/rccm.200504-613PP.
14. Hansand ML, Lowman AM. Biodegradable nanoparticles for drug delivery and targeting. Curr Opin Solid State Mater Sci 2002;6:319–27. doi:10.1016/S1359-0286(02)00117-1.
15. Kawashima Y, Yamamoto H, Takeuchi H, Fujioka S, Hino T. Pulmonary delivery of insulin with nebulized -lactide/glycolide copolymer (PLGA) nanospheres to prolong hypoglycemic effect. J Control Release 1999;62:279–87. doi:10.1016/S0168-3659(99)00048-6.
16. Yamamoto H, Kuno Y, Sugimoto S, Takeuchi H, Kawashima Y. Surface-modified PLGA nanosphere with chitosan improved pulmonary delivery of calcitonin by mucoadhesion and opening of the intercellular tight junctions. J Control Release 2005;102:373–81. doi:10.1016/j.jconrel.2004.10.010.
17. Vaughn JM, McConville JT, Burgess D, Peters JI, Johnston KP, Talbert RL, *et al.* Single dose and multiple dose studies of itraconazole nanoparticles. Eur J Pharm Biopharma 2006;63:95–102. doi:10.1016/j.ejpb.2006.01.006.
18. Dailey LA, Schmehl T, Gessler T, Wittmar M, Grimminger F, Seeger W, *et al.* Nebulization of biodegradable nanoparticles: impact of nebulizer technology and nanoparticle characteristics on aerosol features. J Control Release 2003;86:131–44. doi:10.1016/S0168-3659(02)00370-X.
19. Le Brun PPH, de Boer AH, Frijlink HW, Heijerman HGM. A review of the technical aspects of drug nebulization. Pharm World Sci 2000;22:75–81. doi:10.1023/A:1008786600530.
20. Wendorf J, Singh M, Chesko J, Kazzaz J, Soewanan E, Ugozzoli M, *et al.* A practical approach to the use of nanoparticles for vaccine delivery. J Pharm Sci 2006;95:2738–50. doi:10.1002/jps.20728.
21. Saez A, Guzman M, Molpeceres J, Aberturas MR. Freeze-drying of polycaprolactone and poly(-lactic-glycolic) nanoparticles induce minor particle size changes affecting the oral pharmacokinetics of loaded drugs. Eur J Pharm Biopharma 2000;50:379–87. doi:10.1016/S0939-6411(00)00125-9.
22. Heyder J, Rudolf G. Mathematical models of particle deposition in the human respiratory tract. J Aerosol Sci 1984;15:697–707. doi:10.1016/0021-8502(84)90007-7.
23. Tsapis N, Bennett D, Jackson B, Weitz DA, Edwards DA. Trojan particles: large porous carriers of nanoparticles for drug delivery. Proc Natl Acad Sci U S A 2002;99. doi:10.1073/pnas.182233999.
24. Sung JC, Pulliam BL, Edwards DA. Nanoparticles for drug delivery to the lungs. Trends Biotechnol 2007;25:563–70. doi:10.1016/j.tibtech.2007.09.005.
25. Chew NYK, Shekunov BY, Tong HHY, Chow AHL, Savage C, Wu J, *et al.* Effect of amino acids on the dispersion of disodium cromoglycate powders. J Pharm Sci 2005;94:2289–300. doi:10.1002/jps.20426.
26. Li H-Y, Seville PC, Williamson IJ, Birchall JC. The use of amino acids to enhance the aerosolisation of spray-dried powders for pulmonary gene therapy. J Gene Med 2005;7:343–53. doi:10.1002/jgm.654.
27. Azarmi S, Tao X, Chen H, Wang Z, Finlay WH, Lobenberg R, *et al.* Formulation and cytotoxicity of doxorubicin nanoparticles carried by dry powder aerosol particles. Int J Pharm 2006;319:155–61. doi:10.1016/j.ijpharm.2006.03.052.
28. Hadinoto K, Zhu K, Tan RBH. Drug release study of large hollow nanoparticulate aggregates carrier particles for pulmonary delivery. Int J Pharm 2007;341:195–2061. doi:10.1016/j.ijpharm.2007.03.035.
29. Grenha A, Seijo B, Remunan-Lopez C. Microencapsulated chitosan nanoparticles for lung protein delivery. Eur J Pharm Sci 2005;25:427–37. doi:10.1016/j.ejps.2005.04.009.
30. O'Hara P, Hickey AJ. Respirable PLGA microspheres containing rifampicin for the treatment of tuberculosis: manufacture and characterization. Pharm Res 2000;V17:955–61. doi:10.1023/A:1007527204887.
31. Joshi DP, Lan-Chun-Fung YL, Pritchard JG. Determination of poly (vinyl alcohol) via its complex with boric acid and iodine. Anal Chim Acta 1979;104:153–60. doi:10.1016/S0003-2670(01)83825-3.
32. Garcia-Contreras L, Hickey AJ. Pharmacokinetics of aerosolized rifampicin in the guinea pig. In: Dalby RN, Byron PR, Peart J, Farr S, editors. Respiratory drug delivery VIII. Raleigh, NC: Horwood; 2002.
33. Peloquin CA, Namdar R, Singleton MD, Nix DE. Pharmacokinetics of rifampin under fasting conditions, with food, and with antacids. Chest 1999;115:12–8. doi:10.1378/chest.115.1.12.
34. Garcia-Contreras L, Sethuraman V, Kazantseva M, Godfrey V, Hickey AJ. Evaluation of dosing regimen of respirable rifampicin biodegradable microspheres in the treatment of tuberculosis in the guinea pig. J Antimicrob Chemother 2006;58:980–6. doi:10.1093/jac/dkl369.
35. Suarez S, O'Hara P, Kazantseva M, Newcomer CE, Hopfer R, McMurray DN, *et al.* Respirable PLGA microspheres containing rifampicin for the treatment of tuberculosis: screening in an infectious disease model. Pharm Res 2001;V18:1315–9. doi:10.1023/A:1013094112861.
36. Suarez S, O'Hara P, Kazantseva M, Newcomer CE, Hopfer R, McMurray DN, *et al.* Airways delivery of rifampicin microparticles for the treatment of tuberculosis. J Antimicrob Chemother 2001;48:431–4. doi:10.1093/jac/48.3.431.
37. Coowanitwong I, Arya V, Kulvanich P, Hochhaus GN. Slow release formulations of inhaled rifampin. AAPS J 2008;10:342–8. doi:10.1208/s12248–008–9044–5.
38. Pandey R, Sharma A, Zahoor A, Sharma S, Khuller GK, Prasad B. Poly (DL-lactide-co-glycolide) nanoparticle-based inhalable sustained drug delivery system for experimental tuberculosis. J Antimicrob Chemother 2003;52:981–6. doi:10.1093/jac/dkg477.
39. Sharma A, Sharma S, Khuller GK. Lectin-functionalized poly (lactide-co-glycolide) nanoparticles as oral/aerosolized antitubercular drug carriers for treatment of tuberculosis. J Antimicrob Chemother 2004;54:761–6. doi:10.1093/jac/dkh411.
40. Zahoor A, Sharma S, Khuller GK. Inhalable alginate nanoparticles as antitubercular drug carriers against experimental tuberculosis. Int J Antimicrobial Agents 2005;26:298–303. doi:10.1016/j.ijantimicag.2005.07.012.
41. Esmaeili F, Hosseini-Nasr M, Rad-Malekshahi M, Samadi N, Atyabi F, Dinarvand R. Preparation and antibacterial activity evaluation of rifampicin-loaded poly lactide-co-glycolide nanoparticles. Nanomed Nanotechnol Biol Med 2007;3:161–7. doi:10.1016/j.nano.2007.03.003.
42. Birnbaum DT, Kosmala JD, Brannon-Peppas L. Optimization of preparation techniques for poly(lactic acid-co-glycolic acid) nanoparticles. J Nanopart Res 2000;V2:173–81. doi:10.1023/A:1010038908767.
43. Dailey LA, Jekel N, Fink L, Gessler T, Schmehl T, Wittmar M, *et al.* Investigation of the proinflammatory potential of biodegradable nanoparticle drug delivery systems in the lung. Toxicol Appl Pharmacol 2006;215:100–8. doi:10.1016/j.taap.2006.01.016.
44. Birnbaum DT, Brannon-Peppas L. Molecular weight distribution changes during degradation and release of PLGA nanoparticles containing epirubicin HCl. J Biomater Sci Polym Ed 2003;14:87–102. doi:10.1163/15685620360511155.
45. Peloquin C, Vernon A. Antimycobacterial agents: rifamycins for mycobacterial infections. In: Yu V, Edwards G, McKinnon P, Peloquin C, Morse G, editors. Antimicrobial chemotherapy and vaccines, vol. II: antimicrobial agents. 2nd ed. Pittsburg: Esun Technologies; 2005. p. 383–402.
46. Peloquin C. Clinical pharmacology of the anti-tuberculosis drugs. In: Davies P, Barnes P, Gordon S, editors. Clinical tuberculosis. 4th ed. London: Hodder Arnold; 2008.
47. Dickinson JM, Mitchison DA. Suitability of rifampicin for intermittent administration in the treatment of tuberculosis. Tubercle 1970;51:82–94. doi:10.1016/0041-3879(70)90131-5.